Mitogen-Activated Protein Kinase Kinase Inhibition Enhances Nuclear Proapoptotic Function of p53 in Acute Myelogenous Leukemia Cells

Kensuke Kojima, Marina Konopleva, Ismael J. Samudio, Vivian Ruvolo, and Michael Andreeff

Section of Molecular Hematology and Therapy, Department of Stem Cell Transplantation and Cellular Therapy, M. D. Anderson Cancer Center, The University of Texas, Houston, Texas

Abstract

Activation of the Raf/MEK/ERK pathway and inactivation of wild-type p53 by Mdm2 overexpression are frequent molecular events in acute myelogenous leukemia (AML). We investigated the interaction of Raf/MEK/ERK and p53 pathways after their simultaneous blockades using a selective small-molecule antagonist of Mdm2, Nutlin-3a, and a pharmacologic MEK-specific inhibitor, PD98059. We found that PD98059, which itself has minimal apoptogenic activity, acts synergistically with Nutlin-3a to induce apoptosis in wild-type p53 AML cell lines OCI-AML-3 and MOLM-13. Interestingly, PD98059 enhanced nuclear proapototic function of p53 in these cells. In accordance with the activation of transcription-dependent apoptosis, PD98059 treatment promoted the translocation of p53 from the cytoplasm to the nucleus in OCI-AML-3 cells, in which p53 primarily initiates transcription-independent apoptosis when cells are treated with Nutlin-3a alone. The critical role of p53 localization in cells with increased p53 levels was supported by enhanced apoptosis induction in cells cotreated with Nutlin-3a and the nuclear export inhibitor leptomycin B. PD98059 prevented p53-mediated induction of p21 at the transcriptional level. The repressed expression of antiapototic p21 also seemed to contribute to synergism between PD98059 and Nutlin-3a because (*a*) the synergistic apoptogenic effect was preserved in G_1 cells, (*b*) p53-mediated induction of p21 was preferentially seen in G_1 cells, (*c*) PD98059 strongly antagonized p21 induction by Nutlin-3a, and (*d*) cells with high p21 levels were resistant to apoptosis. This is the first report showing that the Raf/MEK/ERK pathway regulates the subcellular localization of p53 and the relative contribution of transcription-dependent and transcription-independent pathways in p53-mediated apoptosis. [Cancer Res 2007;67(7):3210–9]

Introduction

Malignancies develop when the delicate balance between cell cycle, proliferation, differentiation, and apoptosis is disrupted by genetic and/or environmental cues (1). The Ras-activated Raf/mitogen-activated protein kinase kinase (MEK)/extracellular signal-regulated kinase (ERK) pathway promotes growth and prevents apoptosis of hematopoietic cells, and its constitutive activation has been suggested to play a role in the pathophysiology of acute myelogenous leukemia (AML; ref. 2). We and others have shown constitutive ERK activation in ~70% of clinical AML specimens (3–5). We have shown that treatment of AML blasts with MEK inhibitors PD98059 or PD184352 (CI-1040) inhibits cell growth and proliferation and induces modest apoptosis (3). p53 is a transcription factor that plays an important role in the cellular response to DNA damage either by causing damaged cells to undergo apoptosis or by inducing cell cycle arrest to allow DNA repair (6). p53 is the most frequently inactivated protein in human malignancies, and more than 50% of all solid tumors carry mutations in the *TP53* gene (7). In AML, *TP53* mutations are rare, but inactivation of wild-type p53 protein frequently occurs through overexpression of its negative regulator Mdm2 (8–10). Mdm2 binds p53 at the transactivation domain of p53 and blocks its ability to activate transcription, serves as a ubiquitin ligase that promotes p53 degradation, and furthermore, mediates the nuclear export of p53 (11). Recently, we have reported that the Mdm2 antagonist Nutlin-3a strongly inhibits growth and induces p53-mediated apoptosis in AML (8) and chronic lymphocytic leukemia cells (12).

The Raf/MEK/ERK signaling cascade has been shown to functionally interact with the p53 pathway (13–22). Although details of this interaction are largely unknown, central to the prosurvival effect of the Raf/MEK/ERK signaling on p53 is the up-regulation of Mdm2 (15, 16). Raf/MEK/ERK signaling controls Mdm2 expression by transcriptional activation (15) and positive regulation of the nuclear export of Mdm2 mRNA (16). On the contrary, the Raf/MEK/ERK cascade can induce the expression of $p14^{ARF}$, an Mdm2 antagonist, resulting in p53 activation (15). This can be an important block to cancer progression, and $p14^{ARF}$ expression is lost in various types of malignancies including AML (17, 18). The contradictory induction of $p14^{ARF}$ and Mdm2 seems to account for the Raf/MEK/ERK-dependent attenuation of p53 in the absence of $p14^{ARF}$ or when Mdm2 exceeds that of $p14^{ARF}$ (15). The Raf/MEK/ERK pathway also interferes with p53-dependent cell cycle regulation. Activation of the Raf/MEK/ERK signaling leads to robust induction of the cyclin-dependent kinase inhibitor $p21^{Waf1/Cip1}$ (hereafter referred as p21), whereas its blockade results in reduced expression of p21 (3, 19–22). p21 is one of the major downstream transcriptional targets of p53, which negatively regulates G_1-S transition of the cell cycle (6). p21 has also been shown to be a negative regulator of p53-dependent apoptosis (23).

p53 is a very unstable protein, with a half-life ranging from 5 to 30 min, which is present at low cellular levels owing to continuous degradation largely mediated by Mdm2. p53 activation can be modulated at three levels: (*a*) an increase in p53 concentration by elongated half-life; (*b*) the transformation of the p53 protein from a latent to an active conformation; and (*c*) the translocation of the p53 protein from the cytosol to the nucleus or to the mitochondria (24–26). The transcriptional activation of p53 target genes occurs

Requests for reprints: Michael Andreeff, Section of Molecular Hematology and Therapy, M. D. Anderson Cancer Center, The University of Texas, 1515 Holcombe Boulevard, Unit 448, Houston, TX 77030. Phone: 713-792-7260; Fax: 713-794-4747; E-mail: mandreef@mdanderson.org.

doi:10.1158/0008-5472.CAN-06-2712

in the nucleus. p53 transcriptionally induces the proapoptotic BH3-only proteins Noxa and Puma, which indirectly promote Bax/Bak activation by inhibiting the functions of antiapoptotic Bcl-2 or Bcl-X_L (26). Noxa and Puma are key mediators of p53-induced apoptosis. p53 can also trigger mitochondrial outer membrane permeabilization and apoptosis in the absence of transcription, through direct activation of Bax or Bak or through binding to Bcl-2 or Bcl-X_L (26–28). Although a number of studies have been done to elucidate the modulation of p53 activity at the first two levels, few have addressed the regulation of p53 localization. Recently, we have reported that two distinct mechanisms, transcription-dependent and transcription-independent apoptosis, are both operational in p53-mediated apoptosis in AML cell lines and primary AML cells (8). We have also shown that Mdm2 inhibition–induced p53 primarily executes transcription-dependent and transcription-independent apoptosis in MOLM-13 and OCI-AML-3 cells, respectively (8). In accordance with the difference in mechanism, the nuclear accumulation of p53 was much less pronounced in OCI-AML-3 cells compared with MOLM-13 cells. Because the p53-mediated apoptosis pathway was well preserved in both OCI-AML-3 and MOLM-13 cells, these cells seemed to provide useful models for analyzing an association of the regulation of p53 localization with apoptosis.

In this study, we investigated the molecular events after simultaneous blockade of Raf/MEK/ERK and the p53 pathways in AML cells, to investigate the potential therapeutic utility of this strategy. We found that (*a*) PD98059 promotes translocation of Nutlin-induced p53 from the cytoplasm to the nucleus and enhances transcription-dependent apoptosis and (*b*) PD98059 inhibits p53-dependent induction of p21 in G_1-phase cells, interfering with the p21-mediated cell protection programs against p53-mediated apoptosis.

Materials and Methods

Reagents. The MEK1/2 inhibitor PD98059, the phosphoinositide-3-kinase (PI3K) inhibitor LY294002, and the chromosomal region maintenance 1 (Crm1)–mediated nuclear export inhibitor leptomycin B were purchased from EMD Biosciences (San Diego, CA). Other reagents were obtained as described (8). All compounds except for leptomycin B, which is supplied in 70% methanol, were dissolved in DMSO and kept frozen at −20°C. The final DMSO concentration in the medium did not exceed 0.1% (vol/vol). At this concentration, DMSO itself had no effect up to 72 h on cell growth or viability of the AML cells used in this study. In some experiments, cells were preincubated for 1 h with 3.5 μmol/L cycloheximide or 200 μmol/L Z-VAD-FMK.

Antibodies. The following antibodies were used: rabbit polyclonal anti-p53 (FL-393; Santa Cruz Biotechnology, Santa Cruz, CA); mouse monoclonal anti–phospho-p53 (Ser^{15}; 16G8; Cell Signaling Technology, Beverly, MA); rabbit polyclonal anti–phospho-p53 (Thr^{18}; Cell Signaling Technology); mouse monoclonal anti-Mdm2 (D-12; Santa Cruz Biotechnology); mouse monoclonal anti-p21 (Ab-1; EMD Biosciences); mouse monoclonal anti-p27 (G173-524; BD Biosciences, San Jose, CA); mouse monoclonal anti-Noxa (114C307; EMD Biosciences); rabbit polyclonal anti-Puma (EMD Biosciences); rabbit polyclonal anti-Bax against amino acids 43 to 61 (BD Biosciences); mouse monoclonal anti-Bax (YTH-6A7; Trevigen, Gaithersburg, MD); rabbit polyclonal anti–Bcl-X_L (BD Biosciences); mouse monoclonal anti–Mcl-1 (23; BD Biosciences); rabbit polyclonal anti-survivin (R&D Systems, Minneapolis, MN); rabbit polyclonal anti-p44/42 mitogen-activated protein kinase (MAPK; Cell Signaling Technology); mouse monoclonal anti–phospho-p44/42 MAPK (Cell Signaling Technology); mouse monoclonal anti–Bcl-2 (DAKO Cytomation, Carpinteria, CA); rabbit polyclonal anti–phospho–Bcl-2 (Ser^{70}; Cell Signaling Technology); mouse monoclonal anti–cytochrome *c* oxidase IV (10G8; Molecular Probes, Eugene, OR); rabbit polyclonal anti-Crm1 (Santa Cruz Biotechnology); mouse monoclonal anti–tip associating protein (anti-Tap) (BD Biosciences); and mouse monoclonal anti–β-actin (AC-74; Sigma Chemical Co., St. Louis, MO).

Cell lines and cell cultures. Three human AML cell lines were cultured in RPMI 1640 containing 10% heat-inactivated FCS. OCI-AML-3 and MOLM-13 cells have wild-type p53, whereas p53 is disabled in HL-60 by large deletion of the *TP53* (8). Cell lines were harvested in log-phase growth, seeded at a density of 2×10^5 cells/mL and exposed to the Nutlin-3a and/or PD98059. In experiments involving combinations of Nutlin-3a and PD98059, OCI-AML-3 and HL-60 cells were treated with Nutlin-3a at 0, 1, 2.5, 5, and 10 μmol/L and MOLM-13 cells at 0, 0.4, 1, 2, and 4 μmol/L, in the absence or presence of 20 μmol/L PD98059. The two agents were added simultaneously to cells, and they were cultured for 24 h. Cell viability was evaluated by triplicate counts of trypan blue dye–excluding cells. Experiments were done at least in duplicate.

Annexin V staining. Evaluation of apoptosis by the Annexin V-propidium iodide (PI) binding assay was done as described (8). In some experiments, Annexin V–stained cells were fixed with 2% paraformaldehyde and prepared for cell cycle analysis or intracellular molecule detection as described below.

Cell cycle analysis. Cells were permeabilized in 70% ice-cold ethanol, incubated overnight with PI solution (25 μg/mL PI) and analyzed as described previously (8). Data were gated on the FL2-area versus FL2-width cytogram to exclude doublets and aggregates, and a minimum of 1×10^5 gated cells was collected per sample. Cell cycle distribution was analyzed using ModFit LT software (Verity Software House, Topsham, ME).

Quantitation of intracellular protein by flow cytometry. For intracellular protein detection, cells were fixed with 2% paraformaldehyde, permeabilized with 100% ice-cold methanol, and incubated overnight at 4°C with primary antibodies. For detection of Bax in its active conformation (clone YTH-6A7), cellular fixation and permeabilization was done using the Dako IntraStain kit (DAKO Cytomation), according to manufacturer's instructions. After washing, cells were incubated with Alexa Fluor 488 chicken anti-mouse or anti-rabbit secondary antibodies (Molecular Probes) for 30 min at 4°C. Appropriate isotypic controls were included. If necessary, cells were further stained with PI for simultaneous DNA content analysis.

Western blot analysis. An equal amount of protein lysate was placed on 12% SDS-PAGE for 2 h at 70 V. Proteins were transferred to Hybond-P membranes (Amersham Biosciences, Piscataway, NJ), immunoblotted with appropriate antibodies, and were reacted with enhanced chemiluminescence reagent (Amersham Biosciences). Signals were detected by phosphoimager Storm 860 (Molecular Dynamics, Sunnyvale, CA). An anti–β-actin blot was used in parallel as a loading control. Visualized blots were analyzed by the public-domain NIH image 1.63 program, and protein/β-actin ratios were calculated. All Western blots were done at least in duplicate.

Immunofluorescence and confocal microscopy. Immunofluorescence and confocal microscopic examination was done as previously described (8), with minor modifications. In brief, cells were fixed with 2% paraformaldehyde and permeabilized with ice-cold 100% methanol. The cells were blocked in 5% normal goat serum for 30 min, followed by incubation overnight at 4°C with rabbit polyclonal anti-p53 antibodies FL-393 (1:100 v/v; Santa Cruz Biotechnology) and mouse monoclonal anti–cytochrome *c* oxidase IV (10G8; 1 μg/mL; Molecular Probes). After washing, cells were incubated with Alexa Fluor 488 chicken anti-rabbit secondary antibody and Alexa Fluor 594 chicken anti-mouse secondary antibody (Molecular Probes) diluted in 5% normal goat serum for 30 min at 4°C. Nuclei were counterstained with 4',6-diamidino-2-phenylindole (DAPI).

Real-time quantitative PCR. OCI-AML-3 cells were treated with 20 μmol/L PD98059 and/or 5 μmol/L Nutlin-3a for 3 h. RNA was prepared from cells using RNeasy Mini Kit (Qiagen, Valencia, CA), and first-strand cDNA was generated using random hexamers (SuperScript III First-Strand Synthesis SuperMix; Invitrogen, Carlsbad, CA) from 1 μg total RNA. The mRNA expression levels of p21, Mdm2, Noxa, ABL, and 18S were quantified using TaqMan gene expression assays (Applied Biosystems, Foster City, CA). Quantitative real-time PCR was done using an ABI Prism 7500 Sequence

Detection System and TaqMan Universal Master Mix. The reaction was initiated by a hold for 10 min at 95°C followed by 40 cycles 15 s at 95°C and 1 min at 60°C. Two probes for 18S (Hs99999901_s1) and p21 (Hs00355782_m1) were used. The specificity of the PCR products was confirmed by melting curve analysis with ABI SDS 2.0 software. Relative expression levels were calculated based on the difference in C_T values between the test samples and control untreated cells. This was normalized with expression levels of 18S using the equation $E_{target}(C_{Ttest}^{target} - C_{Tcontrol}^{target})/E_{ref}(C_{Ttest}^{ref} - C_{Tcontrol}^{ref})$. The real-time PCR experiments were carried out in triplicate.

Statistical analysis. The statistical analysis was done using the two-tailed Student's *t* test. Statistical significance was considered when $P < 0.05$. Unless otherwise indicated, average values were expressed as mean ± SD.

Results

Antileukemia activity of Mdm2 antagonists in AML cells is enhanced by combination with MEK inhibitor PD98059. First, we examined the combination effect of the Mdm2 inhibitor Nutlin-3a and the MEK inhibitor PD98059 on the growth and viability of cultured AML cell lines OCI-AML-3 and MOLM-13 that have wild-type p53 and high levels of phosphorylated ERK1/2 (3, 8). As described previously (3), treatment of cells with PD98059 alone showed minimal cytotoxic effect (Fig. 1*A*). Cells were treated with a range of concentrations of PD98059 (1–100 μmol/L). The net increase in the proportion of Annexin V-binding cells was <10%, and the cell viability was determined by trypan blue dye-excluding cells more than 90% even after 48-h exposure of 100 μmol/L PD98059. Next, to determine if MEK inhibition might potentiate cytotoxic effects of Nutlin-3a, we combined 20 μmol/L PD98059 with a range of concentrations of Nutlin-3a. PD98059 at 20 μmol/L sufficiently reduced levels of phosphorylated ERK1/2 in these cells (~50% decrease at 24 h). The interaction study showed a potentiation effect of PD98059 on Nutlin-induced apoptosis (Fig. 1*A*) and growth inhibition (data not shown). The potentiation effect of PD98059 on Nutlin-induced apoptosis seemed higher in OCI-AML-3 cells than in MOLM-13 cells, being consistent with experiments using different concentrations of concomitant Nutlin-3a and PD98059 or their sequential administration with a 3-h interval (data not shown). The sequence Nutlin-3a followed by PD98059 yielded identical results as the reverse sequence. Such a potentiation effect was not seen in p53-defective HL-60 cells (data not shown). The reduced activity of Nutlin-3a and PD98059 combination in MOLM-13 cells may be related to the predominant nuclear localization of p53 in these cells at baseline, as we reported (8).

PD98059 enhances p53-mediated transcription-dependent apoptosis. Because PD98059 itself had minimal apoptogenic effect, we hypothesized that MEK inhibition could actively enhance p53 signaling. Irrespective of transcription-dependent or transcription-independent pathways, p53 signaling activates the proapoptotic protein Bax, resulting in Bax conformational change (29).

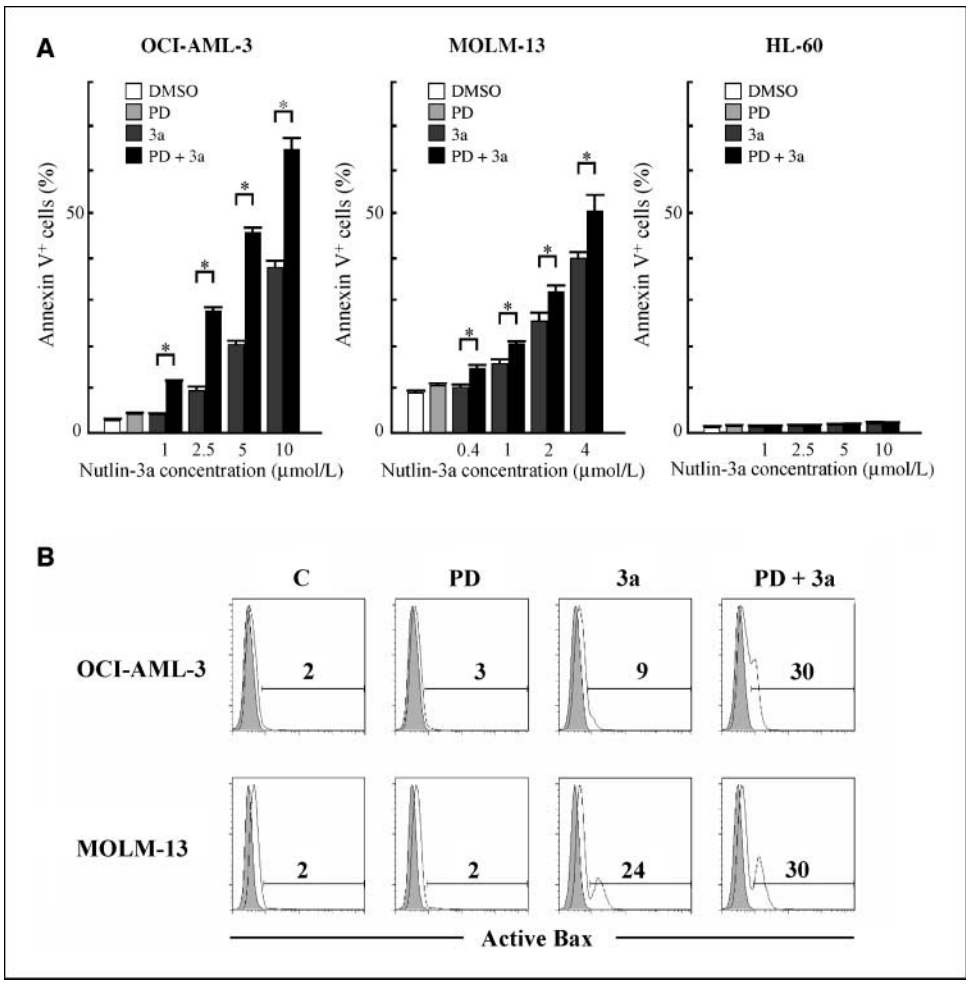

Figure 1. Potentiation effects of PD98059 on p53-mediated apoptosis and Bax activation in AML cells. *A,* PD98059 enhances p53-mediated apoptosis in AML cells. OCI-AML-3, MOLM-13, or HL-60 cells were treated with 20 μmol/L PD98059 (*PD*) and indicated concentrations of Nutlin-3a (*3a*), either as individual agents or in combination, and the annexin V–positive fractions were measured by flow cytometry. *Columns,* mean; *bars,* SD. *, significant at $P < 0.05$. *B,* PD98059 and Nutlin-3a synergistically induce Bax conformational change in OCI-AML-3 and MOLM-13 cells. Cells were treated with 20 μmol/L PD98059 and 5 μmol/L (OCI-AML-3 cells) or 2 μmol/L (MOLM-13 cells) Nutlin-3a for 15 h, either as individual agents or in combination (*PD + 3a*), and Bax conformational change was determined by staining with the active conformation-specific anti-Bax antibody YTH-6A7 or a corresponding isotype control (*shaded*). To block caspase activation-mediated conformational change of Bax, cells were preincubated for 1 h with 200 μmol/L Z-VAD-FMK. Results are representative of three independent experiments.

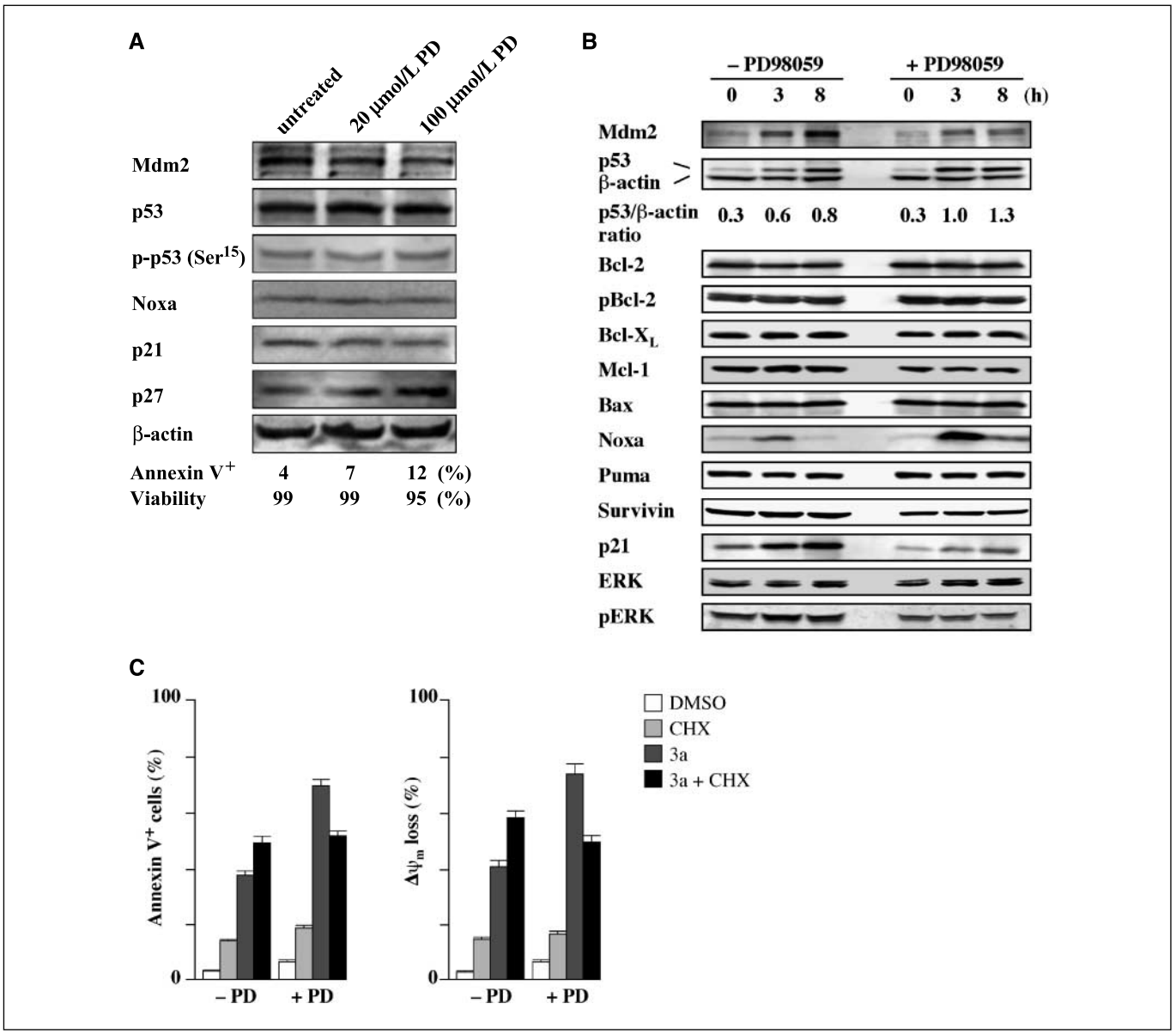

Figure 2. PD98059 prevents p53 from inducing Mdm2 and p21 but not Noxa and enhances transcription-dependent apoptosis in OCI-AML-3 cells. *A,* expression of p53-related proteins and p27 in OCI-AML-3 cells, treated for 24 h with indicated concentrations of PD98059. The effect of PD98059 treatment on expression levels of p53-related proteins was minimal, and an increase in p27 levels was found. *B,* time course expression of p53-related proteins in OCI-AML-3 cells after exposure to 5 μmol/L Nutlin-3a in the absence or presence of 20 μmol/L PD98059. Cells were pretreated with 20 μmol/L PD98059 for 18 h, followed by 8-h treatment of 5 μmol/L Nutlin-3a. Addition of PD98059 enhanced accumulation of p53 and Noxa induction and blunted p53-dependent Mdm2 and p21 up-regulation. *pERK,* p44/42 MAPK (ERK1 and ERK2) dually phosphorylated at Thr^{202} and Thr^{204}; *pBcl-2,* phosphorylated Bcl-2 at Ser^{70}. *C,* OCI-AML-3 cells were cultured for 24 h in the presence of DMSO, 3.5 μmol/L cycloheximide, 10 μmol/L Nutlin-3a, or a combination of cycloheximide and Nutlin-3a. Annexin V–positive fractions and $\Delta\psi_m$ were assessed by flow cytometry. *Columns,* mean of triplicate measurements; *bars,* SD. Comparable results were obtained in two other independent experiments.

Involvement of Bax conformational change was analyzed in OCI-AML-3 cells by means of an antibody directed against the NH_2-terminal region of Bax (clone YTH-6A7). The epitope-specific antibody can react only with Bax in active conformation because the NH_2-terminal region is occluded in unstressed intact cells (30). Cells were preincubated in the presence of 200 μmol/L Z-VAD-FMK before the addition of 20 μmol/L PD98059, 5 μmol/L Nutlin-3a, or both to inhibit caspase activation-mediated Bax cleavage (31). As shown in Fig. 1*B*, few control cells were stained with this antibody (2.2 ± 0.2%), and PD98059 did not induce conformational change of Bax (2.8 ± 0.2%). As predicted, an increase in the percentage of Bax-positive cells was seen following incubation with Nutlin-3a (9.2 ± 0.5%). Interestingly, PD98059 considerably enhanced Bax conformational change by Nutlin-3a (29.8 ± 1.2%), suggesting that MEK inhibition actively enhances the mitochondrial apoptotic pathway. The enhancement of Nutlin-induced Bax conformational change by PD98059 was also seen in MOLM-13 cells, although the effect was less prominent than in OCI-AML-3 cells (Fig. 1*B*). When Bax antibodies directed against amino acids 43 to 61 were used, no differences in the fluorescence pattern between control and drug-treated cells were observed (data not shown).

To clarify the molecular events that contribute to Bax activation, we cultured OCI-AML-3 cells in the presence of 20 or 100 μmol/L PD98059 for 24 h and investigated expression levels of p53-related

proteins and $p27^{Kip1}$ (hereafter referred to as p27). As shown in Fig. 2*A*, p53-related protein levels did not change significantly, whereas PD98059 induced p27. It has been shown that MEK inhibition causes cell cycle arrest at G_1 to p27 induction, respectively (3). Treatment with PD98059 did not induce p53 phosphorylation at Thr^{18} (figure not shown). Next, we investigated time course expression of p53-related proteins in OCI-AML-3 cells after exposure to 5 μmol/L Nutlin-3a in the absence or presence of 18-h preincubation of 20 μmol/L PD98059. Nutlin-3a increased cellular p53 level and induced increased expression of Mdm2, Noxa, and p21 (Fig. 2*B*), as previously reported in detail (8). Interestingly, addition of PD98059 enhanced accumulation of p53 and Noxa induction, whereas it inhibited p53-dependent Mdm2 and p21 up-regulation (Fig. 2*B*). The levels of total and Ser^{70}-phosphorylated Bcl-2 were not affected by the presence of PD98059, suggesting a minor role of Bcl-2 in the enhancement of Nutlin-induced apoptosis (32). PD98059 pretreatment resulted in reduced levels of Mcl-1 and survivin (Fig. 2*B*), in accordance with previous reports (3, 33). We have shown that PD98059-induced repression of survivin expression occurs at the level of transcription (33). Although p53 has also been reported to repress the survivin promoter (34), the levels of survivin did not decrease further by the addition of Nutlin-3a to PD98059 (Fig. 2*B*).

We have shown that Nutlin-3a induces transcription-independent apoptosis in OCI-AML-3 cells (8). The role of newly synthesized proteins in the initiation of apoptosis was addressed by the treatment of OCI-AML-3 cells with PD98059 and Nutlin-3a in the absence or presence of 3.5 μmol/L cycloheximide. Inhibition of protein synthesis with cycloheximide did not rescue OCI-AML-3 from Annexin V induction or $\Delta\psi_m$ loss by Nutlin-3a (Fig. 2*C*), as we have reported previously (8). Interestingly, when Nutlin-3a was combined with PD98059, cycloheximide partially protected cells

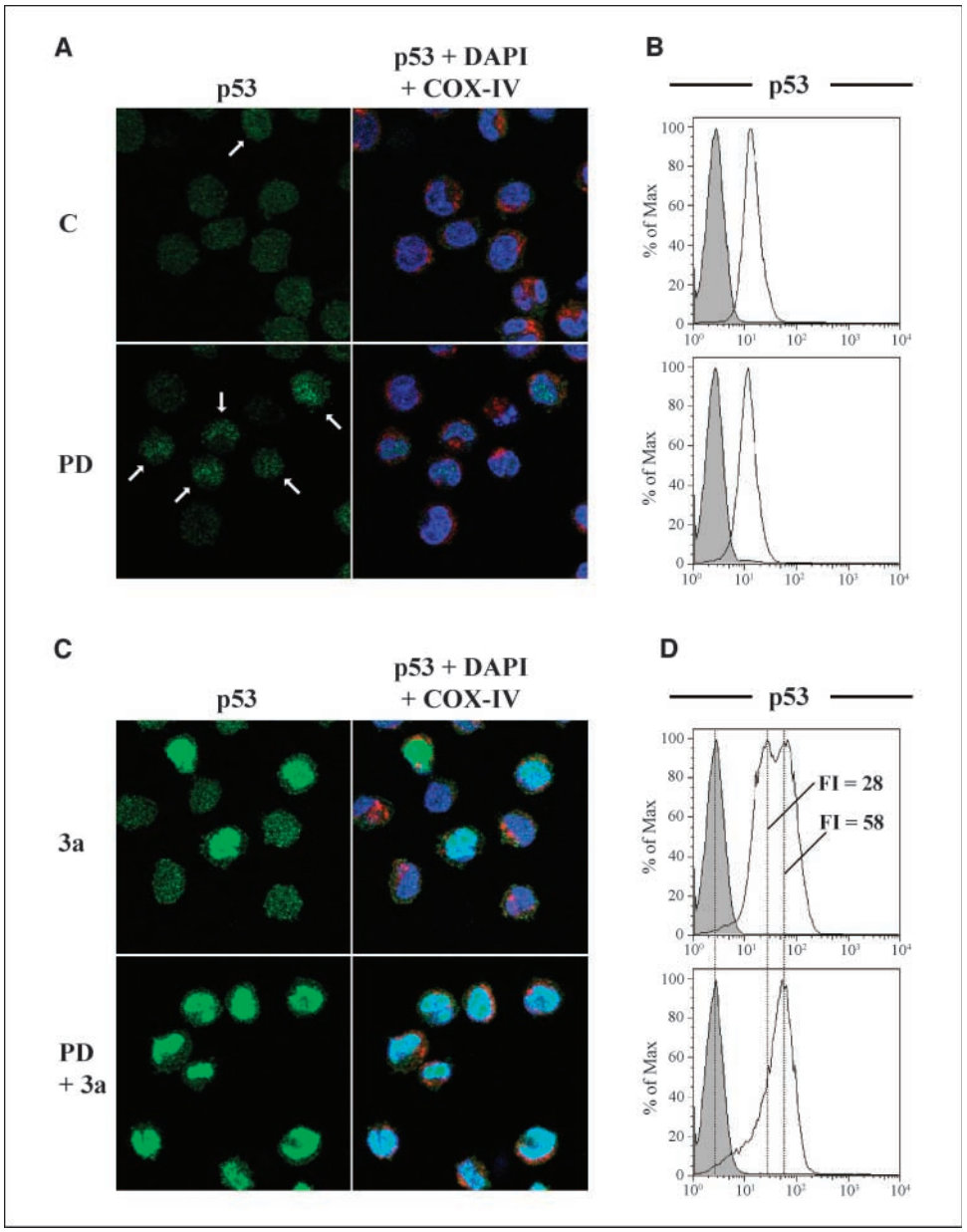

Figure 3. PD98059 promotes the translocation of p53 from the cytoplasm to the nucleus. *A* and *B,* OCI-AML-3 cells were cultured with or without 20 μmol/L PD98059 (*PD* or *C*) for 24 h. *A,* cells were fixed, stained for p53 (green), and mitochondrial marker protein cytochrome *c* oxidase IV (*COX-IV*; *red*) and visualized by confocal microscopy. Nuclei were counterstained with DAPI (*blue*). *Arrows*, cells with preferential p53 localization to the nucleus. *C* and *D,* OCI-AML-3 cells were pretreated with 20 μmol/L PD98059 for 18 h, followed by 6-h treatment of 5 μmol/L Nutlin-3a. Cells treated with Nutlin-3a alone for 6 h served as controls. PD98059 promoted the translocation of Nutlin-induced p53 from the cytoplasm to the nucleus and increased cellular levels of p53. *FI,* fluorescence intensity.

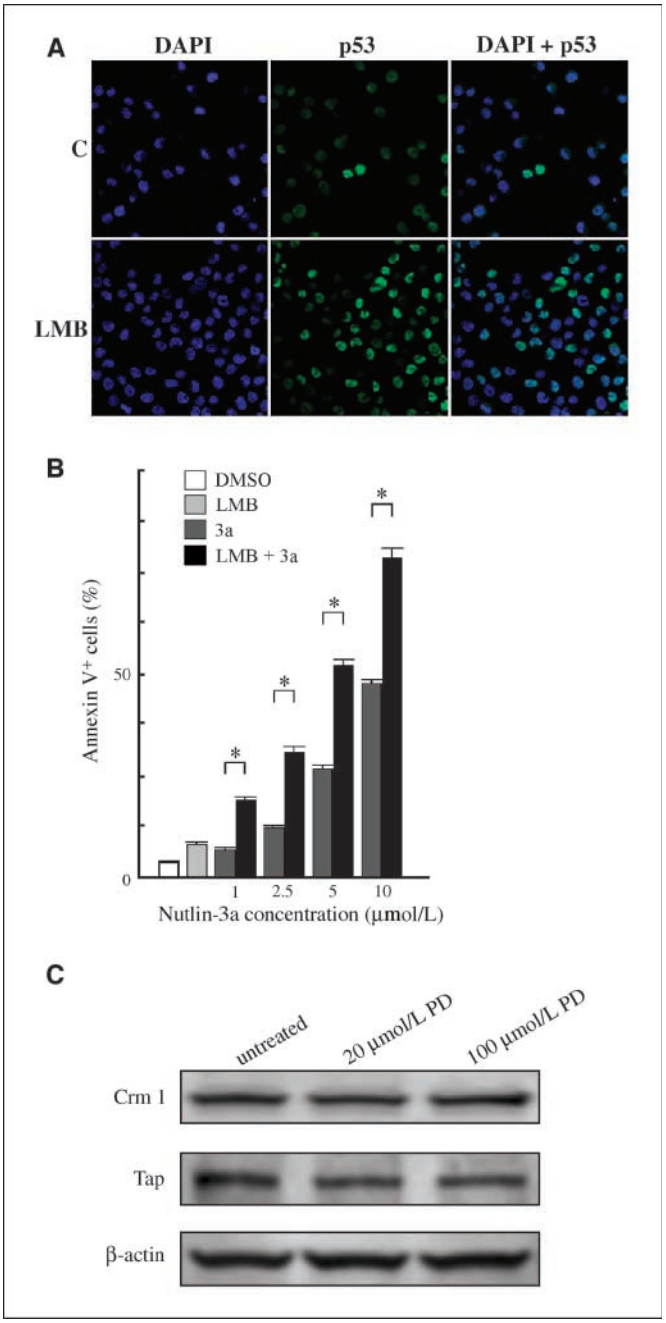

Figure 4. *A,* leptomycin B accumulates p53 into the nucleus of OCI-AML-3 cells. Localization of p53 after leptomycin B treatment. Cells were treated with 0.5 ng/mL leptomycin B for 3 h, and untreated (*C*) or treated (*LMB*) cells were stained for p53 (*green*) and visualized by confocal microscopy. Nuclei were counterstained with DAPI. *B,* Leptomycin B induces apoptosis in synergy with Nutlin-3a. Cells were incubated for 24 h with indicated concentrations of Nutlin-3a in the absence or presence of 0.5 ng/mL leptomycin B, and the annexin V–positive fractions were measured by flow cytometry. *Columns,* mean; *bars,* SD. *, significant at $P < 0.05$. *C,* expression of nuclear exporter Crm1 and Tap in OCI-AML-3 cells, treated for 24 h with 100 μmol/L PD98059. The effect of PD98059 treatment on their expression levels was minimal.

from both Annexin V induction and $\Delta\psi_m$ loss (Fig. 2*C*). The cycloheximide experiment was also done in MOLM-13 cells, in which p53 primarily induces transcription-dependent apoptosis. The inhibitory effect of cycloheximide pretreatment on loss of $\Delta\psi_m$ in MOLM-13 cells treated with Nutlin-3a and PD98059 compared with Nutlin-3a alone increased from 28% to 43%. Our findings suggest that PD98059 can enhance transcription-dependent apoptotic signaling of the p53 pathway in these AML cell lines.

MEK inhibition accumulates p53 into the nucleus in OCI-AML-3 cells. To investigate if PD98059 can mediate subcellular localization of wild-type p53, we determined p53 localization in OCI-AML-3 cells that were treated with PD98059 in the absence or presence of Nutlin-3a using confocal microscopy. As previously reported, a small amount of p53 was diffusely distributed in untreated OCI-AML-3 cells, and after Nutlin-3a treatment, cells exhibited increased p53 staining with inconspicuous accumulation in the nucleus (8). After 24-h exposure to 20 μmol/L PD98059 alone, the percentage of cells with preferential nuclear localization of p53 was significantly increased to 18.8 ± 2.1% (untreated control: 7.1 ± 0.6%; $P < 0.01$) although the incidence in the total cell population was still low (Fig. 3*A*). Treatment with 20 μmol/L PD98059 itself neither triggered significant apoptosis (Fig. 1*A*) nor increased p53 levels (Figs. 2*A* and 3*B*). Next, we investigated if PD98059 could mediate p53 localization in cells simultaneously treated with 5 μmol/L Nutlin-3a. The percentage of cells with nuclear p53 accumulation in cotreated cells (71.7 ± 4.2%) was significantly higher than in cells treated with Nutlin-3a alone (39.1 ± 2.6%; $P < 0.01$; Fig. 3*C*). Flow cytometric quantitation of intracellular p53 revealed a bimodal distribution in cells treated with Nutlin-3a alone that converted into a unimodal high peak when cells were treated with Nutlin-3a and PD98059 (Fig. 3*D*). The fluorescence intensity of the merged peak was almost identical to that of the higher peak in cells treated with Nutlin-3a alone. Because cells with nuclear p53 localization showed abundant p53, PD98059-mediated nuclear accumulation of p53 seemed not only to support direct transcriptional activation of numerous p53 target genes but to protect p53 from degradation. The PI3K pathway is another signal transduction pathway that is activated by Ras, and the Raf/MEK/ERK and the PI3K pathways have been described to cooperate to promote oncogenic transformation of mammalian cells (21, 35). To see if the blockade of the PI3K pathway could mediate p53 localization or cellular p53 levels, OCI-AML-3 cells were treated with the PI3K inhibitor LY294002 (20 μmol/L) in the absence or presence of 5 μmol/L Nutlin-3a. LY294002 did not induce nuclear accumulation of p53. Furthermore, LY294002 treatment of cells reduced basal p53 levels and inhibited p53 induction by Nutlin-3a (figure not shown), which was in clear contrast with the synergistic p53 induction by PD98059 and Nutlin-3a. The inhibitory effect of LY294002 on p53 induction has recently been reported in cells treated with DNA-damaging agents (36). The nuclear relocation of p53 and its increased levels in relation to PD98059 treatment were inconspicuous in MOLM-13 cells (data not shown), in which Nutlin-3a alone causes intense nuclear accumulation of p53 (8).

Nuclear p53 accumulation by leptomycin B works in synergy with Nutlin-3a to induce apoptosis in OCI-AML-3 cells. We hypothesized that the ability of PD98059 to accumulate p53 into the nucleus allowed it to synergistically act with Nutlin-3a in OCI-AML-3 cells. To determine if nuclear accumulation of p53 is sufficient to potentiate Nutlin-induced apoptosis, we used a potent inhibitor of Crm1-mediated nuclear export, leptomycin B, to mimic the nuclear p53 accumulation by PD98059. OCI-AML-3 cells were incubated with a range of concentrations of Nutlin-3a for 24 h, in the absence or presence of 0.5 ng/mL leptomycin B. Treatment with leptomycin B alone caused nuclear accumulation of p53 (Fig. 4*A*), inducing modest apoptosis (6.5 ± 0.4%; untreated control: 3.0 ± 0.2%; Fig. 4*B*). The addition of leptomycin B to

Nutlin-3a resulted in an impressive increase in the percentage of Annexin V–positive cells compared with cells treated with Nutlin-3a alone (41.8 ± 1.2% versus 21.6 ± 0.6% at 5 μmol/L Nutlin-3a; Fig. 4*B*), suggesting that nuclear accumulation of p53 can enhance Nutlin-induced apoptosis in OCI-AML-3 cells.

MEK inhibition does not affect the nucleoplasmic localization of Mdm2. Mdm2 is one of the key mediators of p53 nuclear export (11), and we showed that PD98059 attenuates both basal levels of Mdm2 and p53-dependent Mdm2 induction after Nutlin-3a treatment. Because it has been described that the localization of Mdm2 could affect p53 localization (37, 38), we determined the Mdm2 localization in OCI-AML-3 cells treated with 20 μmol/L PD98059 in the absence or presence of 5 μmol/L Nutlin-3a, using confocal microscopy. Cells under unstressed conditions showed nucleoplasmic distribution of Mdm2, which was not affected by Nutlin-3a or PD98059 treatment (figure not shown), arguing against the idea that the MEK inhibition stabilizes p53 by blocking nucleocytoplasmic shuttling of Mdm2 or by sequestering Mdm2 in the nucleolus. Protein levels of Crm1 (39) or Tap (40), which could mediate nuclear export of p53 in an Mdm2-independent manner, were not affected by 24-h treatment of OCI-AML-3 cells with 100 μmol/L PD98059, as evidenced by Western blotting (Fig. 4*C*).

PD98059 restricts p21-mediated antiapoptotic mechanisms by repressing p53-dependent induction of p21, which enables Nutlin-3a to induce sufficient apoptosis in G_1-phase cells. To clarify if the apoptotic potential of Nutlin-3a is consistently

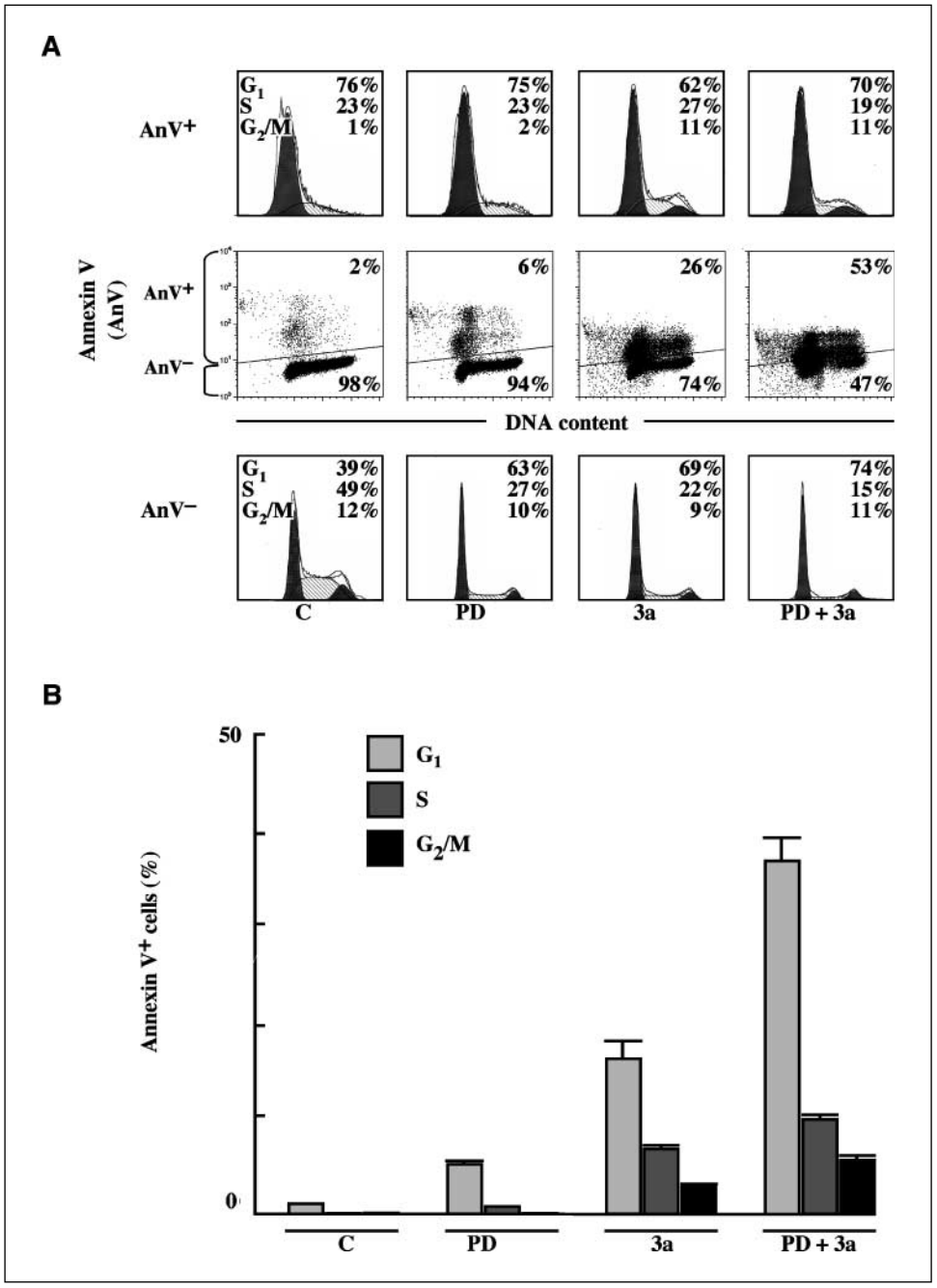

Figure 5. MEK inhibition enhances apoptosis induction by Nutlin-3a, which is most prominent in G_1 cells. OCI-AML-3 cells were treated with 20 μmol/L PD98059 and 5 μmol/L Nutlin-3a for 24 h, either as individual agents or in combination (*P* + *D*). *A,* annexin V–positive (*AnV*$^+$) and annexin V–negative (*AnV*$^-$) fractions in correlation with DNA content were measured by flow cytometry. Data were gated on the FL2-area versus FL2-width cytogram to exclude doublets. Cells were gated on dot plots (*middle row*) based on Annexin staining. Histograms indicate the distribution of DNA content in the gated populations (AnV$^+$: *top row*; or AnV$^-$: *bottom row*) of the preceding dot plots. Results are representative of three independent experiments. *B,* the percentages of annexin V–positive cells in total cells. *Columns,* mean; *bars,* SD.

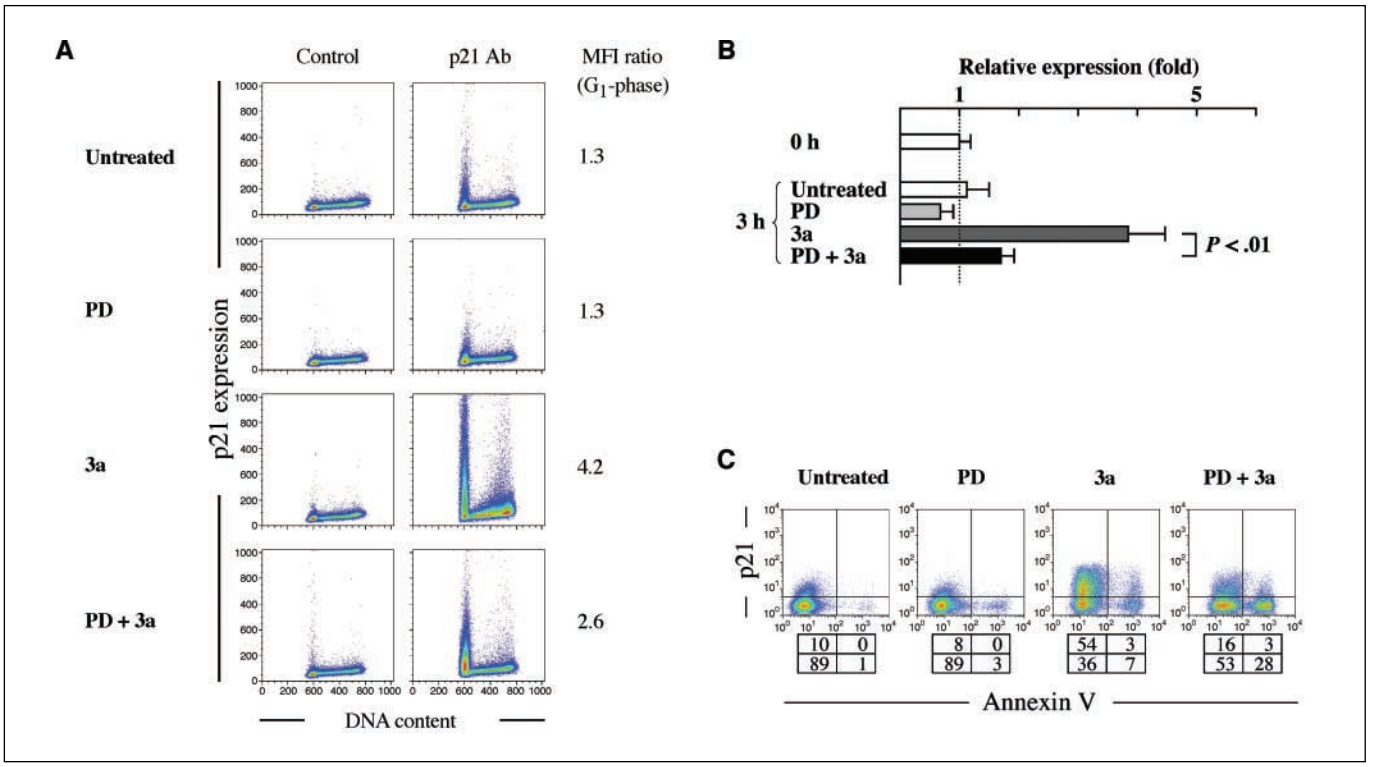

Figure 6. PD98059 inhibits p53-mediated induction of p21 by Nutlin-3a, and cells expressing p21 are resistant to Nutlin-induced apoptosis. *A,* OCI-AML-3 cells were treated with 20 μmol/L PD98059 and 5 μmol/L Nutlin-3a for 8 h, either as individual agents or in combination, and p21 expression levels and DNA content were measured by flow cytometry. To block caspase activation-mediated p21 cleavage, cells were preincubated for 1 h with 200 μmol/L Z-VAD-FMK. Induction of p21 by Nutlin-3a was most prominent in G_1 cells, which was antagonized by PD98059 treatment. Mean fluorescence intensity (*MFI*) ratio in G_1 cells was calculated by the formula: MFI ratio (G_1-phase) = (MFI of G_1 cells stained with anti-p21 antibody)/(MFI of isotypic control-stained G_1 cells). *B,* OCI-AML-3 cells were treated with 20 μmol/L PD98059 and 5 μmol/L Nutlin-3a for 3 h, either as individual agents or in combination, and p21 transcripts were quantitated by real-time reverse transcription-PCR. Each real-time PCR was done in triplicate, and the average fold induction relative to time 0 was shown with SD. *C,* OCI-AML-3 cells were treated with 20 μmol/L PD98059 and 5 μmol/L Nutlin-3a for 24 h, either as individual agents or in combination, and annexin V–positive fractions in correlation with p21 expression levels were measured by flow cytometry. To block caspase activation-mediated p21 cleavage, cells were preincubated for 1 h with 200 μmol/L Z-VAD-FMK. Because of considerable induction of p21 at 24 h, data on p21 expression levels were plotted on logarithmic scale. Results show that cells with induced p21 were mostly negative for annexin V.

enhanced by combination with PD98059 in different phases of cell cycle, OCI-AML-3 cells were treated with 20 μmol/L PD98059 and 5 μmol/L Nutlin-3a, either as individual agents or in combination. As shown in Fig. 5*A*, both PD98059 and Nutlin-3a caused profound G_1-phase cell cycle arrest in nonapoptotic cells (AnV^-), which was further enhanced by their combination. We and others have shown that PD98059 and Nutlin-3a induce G_1 arrest through p27 and p21 induction, respectively (3, 8, 21, 22, 41). In contrast to the modest apoptosis in PD98059-treated cells, Nutlin-3a induced significant apoptosis independent of cell cycle phases, with a relatively sparing effect on G_1 cells (Fig. 5*A*). Interestingly, the synergistic apoptotic effect between PD98059 and Nutlin-3a was preserved in G_1-phase cells (Fig. 5*B*), suggesting that p53-dependent G_1 cell cycle arrest does not efficiently protect cells from apoptosis in dually treated cells. We have recently found that p53-dependent induction of p21 is preferentially seen in G_1 cells (42). Because p21 has been described to inhibit p53-dependent apoptosis (23), we investigated if the inhibitory effect of PD98059 on p53-mediated p21 induction could contribute to the enhanced apoptosis induction in cells treated with PD98059 and Nutlin-3a. As shown in Fig. 6*A*, 20 μmol/L PD98059 strongly antagonized p21 induction by Nutlin-3a. Furthermore, cells with high p21 expression were resistant to apoptosis induced by Nutlin-3a alone and by Nutlin-3a and PD98059 (Fig. 6*B*), suggesting a protective role of p21 in p53-dependent apoptosis. Taken together, the synergistic apoptotic effect between PD98059 and Nutlin-3a is, to some degree, attributable to the inhibitory effect of PD98059 on p53-dependent p21 induction.

Discussion

Nutlins prevent p53 from binding to its negative regulator Mdm2, leading to effective stabilization of p53 and activation of the p53 pathway *in vitro* and *in vivo* (41). We have shown that Nutlins effectively induce p53-dependent apoptosis in AML, in which *TP53* mutations are rare and Mdm2 overexpression is a frequent event (8). Because Mdm2 itself is the product of a p53-inducible gene, however, the negative feedback loop may limit the duration or amplitude of p53-mediated apoptosis in AML cells after Nutlin treatment. In the majority of primary AML cases, the Raf/MEK/ERK pathway is constitutively activated (3–5) and prognostic (43). Because Raf/MEK/ERK signaling has been shown to up-regulate Mdm2 expression (15, 16), we investigated if the blockade of this pathway can potentiate Nutlin-induced p53-mediated apoptosis and found that the MEK inhibitor PD98059 prevents p53-dependent Mdm2 induction and synergizes with Mdm2 inhibitor Nutlin-3a to induce apoptosis in AML cell lines. Importantly, MEK inhibition promoted translocation of p53 from the cytoplasm to the nucleus and enhanced transcription-dependent apoptosis in

Nutlin-treated OCI-AML-3 cells, in which p53 primarily induces transcription-independent apoptosis when cells are treated with Nutlin-3a alone (8). The regulation of p53 localization in association with Raf/MEK/ERK signaling has not been investigated. In support of the idea that interference with p53 localization enhances p53 activation in Nutlin-treated cells, combining Nutlin-3a with the nuclear export inhibitor leptomycin B, which was by itself only minimally apoptogenic, resulted in considerable apoptosis in OCI-AML-3 cells. Because neither blockade of Mdm2-p53 interaction nor MEK inhibition has been shown to cause posttranslational modifications of p53 toward activation (25, 44), our findings suggest that the two independent p53 responses, including an increase in p53 levels and nuclear relocation of p53, could cooperate to activate p53 signaling. We also suggest that the nuclear translocation of p53 could play a role in p53 stabilization as well as transcriptional activation of p53 target genes, at least in some AML cells, because OCI-AML-3 cells with the nuclear localization of p53 showed high levels of p53.

The regulation of p53 nucleocytoplasmic shuttling is poorly understood, but there have been several proteins that influence p53 nuclear import and export, one of the most important being Mdm2 (39). Mdm2 is involved in the nuclear export of p53, for which Mdm2 ubiquitin ligase activity is required (45). The function of Mdm2 has been directly linked to the nuclear exclusion of p53 in a subset of tumors such as neuroblastoma and breast cancer, in which inhibition of Mdm2 expression by an antisense oligonucleotide or inhibition of Mdm2 function by overexpressed $p14^{ARF}$ results in a relocation of p53 from the cytoplasm to the nucleus (46). The vital role of Mdm2 in the regulation of p53 nucleocytoplasmic shuttling is further emphasized by the fact that most of the reported proteins regulate p53 localization by interfering with Mdm2 (37, 38, 45–48). It is therefore possible that the down-regulation of Mdm2 after PD98059 treatment could contribute to the nuclear accumulation of p53 and the enhancement of transcription-dependent apoptosis. On the other hand, we have previously shown that the blockade of Mdm2-p53 interaction by Nutlin-3a does not always result in the accumulation of p53 in the nucleus and may induce its mitochondrial relocation in AML cells (8). Further investigations are needed to clarify if the extent of Mdm2 inhibition could affect the subcellular localization of p53 and if Raf/MEK/ERK signaling can regulate p53 localization in an Mdm2-independent manner.

The downstream events mediated by p53 take place by two major pathways: cell cycle arrest and apoptosis. p53-dependent cell cycle arrest is primarily mediated by the cyclin-dependent kinase inhibitor p21. It is not clear how an individual cell chooses between p21-dependent cell cycle arrest and apoptosis after activation of p53, but p53-inducible p21 has been reported to interfere with p53-dependent apoptosis (23, 49–51). Direct mechanisms by which p21 inhibits apoptosis include inhibition of initiator caspase-8 cleavage (49), interaction with procaspase-3 masking the serine proteinase-cleaving site (50), and stabilization of the apoptotic inhibitor protein c-IAP1 (51). In contrast, there have also been reports suggesting a proapototic function of p21 under certain conditions in specific systems (52). Using the highly specific inhibitors PD98059 and Nutlin-3a, we found that MEK inhibition can block p53-dependent p21 induction, which takes place most prominently in G_1 cells. Because high levels of p21 expression protected cells from apoptosis induced by combination treatment with PD98059 and Nutlin-3a as well as by Nutlin-3a alone, the inhibitory effect of PD98059 on p53-mediated p21 induction seemed to contribute to the enhanced apoptosis induction in dually treated cells. Further identification of factors that specifically repress p21 would provide a better understanding of its role in cancer and may sensitize cancer cells to current chemotherapeutic agents that activate p53 signaling (53).

Acknowledgments

Received 7/21/2006; revised 12/14/2006; accepted 1/17/2007.

Grant support: NIH (AML-PO1) CA55164, CA49639, CA89346 and CA16672 and the Paul and Mary Haas Chair in Genetics (M. Andreeff) and by the Kanae Foundation for Life and Socio-Medical Science (2004), the Mochida Memorial Foundation for Medical and Pharmaceutical Research (2004), and Uehara Memorial Foundation (2004; K. Kojima).

The costs of publication of this article were defrayed in part by the payment of page charges. This article must therefore be hereby marked *advertisement* in accordance with 18 U.S.C. Section 1734 solely to indicate this fact.

The authors acknowledge Dr. Lyubomir T. Vassilev of Hoffmann-La Roche, Nutley, NJ, for kindly providing Nutlin-3a and for stimulating discussions; Dr. Yoshinobu Matsuo of Fujisaki Cell Center, Hayashibara Hayashibara Biochemical Laboratories, Okayama, Japan, for MOLM-13 cells; and Rosemarie B. Lauzon for her assistance with the manuscript.

References

1. Hanahan D, Weinberg RA. The hallmarks of cancer. Cell 2000;100:57–70.
2. Platanias LC. Map kinase signaling pathways and hematologic malignancies. Blood 2003;101:4667–79.
3. Milella M, Kornblau SM, Estrov Z, et al. Therapeutic targeting of the MEK/MAPK signal transduction module in acute myeloid leukemia. J Clin Invest 2001;108:851–9.
4. Kim SC, Hahn JS, Min YH, Yoo NC, Ko YW, Lee WJ. Constitutive activation of extracellular signal-regulated kinase in human acute leukemias: combined role of activation of MEK, hyperexpression of extracellular signal-regulated kinase, and downregulation of a phosphatase, PAC1. Blood 1999;93:3893–9.
5. Towatari M, Iida H, Tanimoto M, Iwata H, Hamaguchi M, Saito H. Constitutive activation of mitogen-activated protein kinase pathway in acute leukemia cells. Leukemia 1997;11:479–84.
6. Vousden KH, Lu X. Live or let die: the cell's response to p53. Nat Rev Cancer 2002;2:594–604.
7. Hollstein M, Sidransky D, Vogelstein B, Harris CC. p53 mutations in human cancers. Science 1991;253:49–53.
8. Kojima K, Konopleva M, Samudio IJ, et al. MDM2 antagonists induce p53-dependent apoptosis in AML: implications for leukemia therapy. Blood 2005;106:3150–9.
9. Faderl S, Kantarjian HM, Estey E, et al. The prognostic significance of $p16^{INK4a}/p14^{ARF}$ locus deletion and MDM-2 protein expression in adult acute myelogenous leukemia. Cancer 2000;89:1976–82.
10. Bueso-Ramos CE, Yang Y, deLeon E, McCown P, Stass SA, Albitar M. The human MDM-2 oncogene is overexpressed in leukemias. Blood 1993;82:2617–23.
11. Michael D, Oren M. The p53-2 module and the ubiquitin system. Semin Cancer Biol 2003;13:49–58.
12. Kojima K, Konopleva M, McQueen T, O'Brien S, Plunkett W, Andreeff M. Mdm2 inhibitor Nutlin-3a induces p53-mediated apoptosis by transcription-dependent and transcription-independent mechanisms and may overcome Atm-mediated resistance to fludarabine in chronic lymphocytic leukemia. Blood 2006;108:993–1000.
13. Wu GS. The functional interactions between the p53 and MAPK signaling pathways. Cancer Biol Ther 2004;3:156–61.
14. Deng X, Ruvolo P, Carr B, May WS, Jr. Survival function of ERK1/2 as IL-3–activated, staurosporine-resistant Bcl2 kinases. Proc Natl Acad Sci U S A 2000;97:1578–83.
15. Ries S, Biederer C, Woods D, et al. Opposing effects of Ras on p53: transcriptional activation of mdm2 and induction of p19ARF. Cell 2000;103:321–30.
16. Phelps M, Phillips A, Darley M, Blaydes JP. MEK-ERK signaling controls Hdm2 oncoprotein expression by regulating hdm2 mRNA export to the cytoplasm. J Biol Chem 2005;280:16651–8.
17. Taniguchi T, Chikatsu N, Takahashi S, et al. Expression of $p16^{INK4A}$ and $p14^{ARF}$ in hematological malignancies. Leukemia 1999;13:1760–9.
18. Linggi B, Muller-Tidow C, van de Locht L, et al. The t(8;21) fusion protein, AML1 ETO, specifically represses the transcription of the $p14^{ARF}$ tumor suppressor in acute myeloid leukemia. Nat Med 2002;8:743–50.
19. Sewing A, Wiseman B, Lloyd AC, Land H. High-intensity Raf signal causes cell cycle arrest mediated by $p21^{Cip1}$. Mol Cell Biol 1997;17:5588–97.
20. Woods D, Parry D, Cherwinski H, Bosch E, Lees E, McMahon M. Raf-induced proliferation or cell cycle arrest is determined by the level of Raf activity with arrest mediated by $p21^{Cip1}$. Mol Cell Biol 1997;17:5598–611.

21. Mirza AM, Gysin S, Malek N, Nakayama K, Roberts JM, McMahon M. Cooperative regulation of the cell division cycle by the protein kinases RAF and AKT. Mol Cell Biol 2004;24:10868–81.

22. Coleman ML, Marshall CJ, Olson MF. Ras promotes $p21^{Waf1/Cip1}$ protein stability via a cyclin D1-imposed block in proteasome-mediated degradation. EMBO J 2003;22:2036–46.

23. Gartel AL, Tyner AL. The role of the cyclin-dependent kinase inhibitor p21 in apoptosis. Mol Cancer Ther 2002;1:639–49.

24. Moll UM, Petrenko O. The MDM2–53 interaction. Mol Cancer Res 2003;1:1001–8.

25. Bode AM, Dong Z. Post-translational modification of p53 in tumorigenesis. Nat Rev Cancer 2004;4:793–805.

26. Schuler M, Green DR. Transcription, apoptosis and p53: catch-22. Trends Genet 2005;21:182–7.

27. Mihara M, Erster S, Zaika A, et al. p53 has a direct apoptogenic role at the mitochondria. Mol Cell 2003;11:577–90.

28. Chipuk JE, Kuwana T, Bouchier-Hayes L, et al. Direct activation of Bax by p53 mediates mitochondrial membrane permeabilization and apoptosis. Science 2004;303:1010–4.

29. Chipuk JE, Bouchier-Hayes L, Kuwana T, Newmeyer DD, Green DR. PUMA couples the nuclear and cytoplasmic proapoptotic function of p53. Science 2005;309:1732–5.

30. Desagher S, Osen-Sand A, Nichols A, et al. Bid-induced conformational change of Bax is responsible for mitochondrial cytochrome *c* release during apoptosis. J Cell Biol 1999;144:891–901.

31. Bellosillo B, Villamor N, Lopez-Guillermo A, et al. Spontaneous and drug-induced apoptosis is mediated by conformational changes of Bax and Bak in B-cell chronic lymphocytic leukemia. Blood 2002;100:1810–6.

32. Tamura Y, Simizu S, Osada H. The phosphorylation status and anti-apoptotic activity of Bcl-2 are regulated by ERK and protein phosphatase 2A on the mitochondria. FEBS Lett 2004;569:249–55.

33. Carter BZ, Milella M, Altieri DC, Andreeff M. Cytokine-regulated expression of survivin in myeloid leukemia. Blood 2001;97:2784–90.

34. Hoffman WH, Biade S, Zilfou JT, Chen J, Murphy M. Transcriptional repression of the anti-apoptotic survivin gene by wild-type p53. J Biol Chem 2002;277:3247–57.

35. Jones SM, Kazlauskas A. Growth-factor–dependent mitogenesis requires two distinct phases of signalling. Nat Cell Biol 2001;3:165–72.

36. Bar J, Lukaschuk N, Zalcenstein A, Wilder S, Seger R, Oren M. The PI3K inhibitor LY294002 prevents p53 induction by DNA damage and attenuates chemotherapy-induced apoptosis. Cell Death Differ 2005;12:1578–87.

37. Tao W, Levine AJ. $P19^{ARF}$ stabilizes p53 by blocking nucleo-cytoplasmic shuttling of Mdm2. Proc Natl Acad Sci U S A 1999;96:6937–41.

38. Mayo LD, Donner DB. A phosphatidylinositol 3-kinase/Akt pathway promotes translocation of Mdm2 from the cytoplasm to the nucleus. Proc Natl Acad Sci U S A 2001;98:11598–603.

39. O'Brate A, Giannakakou P. The importance of p53 location: nuclear or cytoplasmic zip code? Drug Resist Updat 2003;6:313–22.

40. O'Hagan HM, Ljungman M. Efficient NES-dependent protein nuclear export requires ongoing synthesis and export of mRNAs. Exp Cell Res 2004;297:548–59.

41. Vassilev LT, Vu BT, Graves B, et al. *In vivo* activation of the p53 pathway by small-molecule antagonists of MDM2. Science 2004;303:844–8.

42. Kojima K, Konopleva M, Samudio IJ, Schober WD, Bornmann WG, Andreeff M. Concomitant inhibition of MDM2 and Bcl-2 protein function synergistically induce mitochondrial apoptosis in AML. Cell Cycle 2006;5:2778–86.

43. Kornblau SM, Womble M, Qiu YH, et al. Simultaneous activation of multiple signal transduction pathways confers poor prognosis in acute myelogenous leukemia. Blood 2006;108:2358–65.

44. Thompson T, Tovar C, Yang H, et al. Phosphorylation of p53 on key serines is dispensable for transcriptional activation and apoptosis. J Biol Chem 2004;279:53015–22.

45. Li M, Brooks CL, Wu-Baer F, Chen D, Baer R, Gu W. Mono- versus polyubiquitination: differential control of p53 fate by Mdm2. Science 2003;302:1972–5.

46. Lu W, Pochampally R, Chen L, Traidej M, Wang Y, Chen J. Nuclear exclusion of p53 in a subset of tumors requires MDM2 function. Oncogene 2000;19:232–40.

47. Goldberg Z, Vogt Sionov R, Berger M, et al. Tyrosine phosphorylation of Mdm2 by c-Abl: implications for p53 regulation. EMBO J 2002;21:3715–27.

48. den Besten W, Kuo ML, Williams RT, Sherr CJ. Myeloid leukemia-associated nucleophosmin mutants perturb p53-dependent and independent activities of the Arf tumor suppressor protein. Cell Cycle 2005;4:1593–8.

49. Xu SQ, El-Deiry WS. $p21^{WAF1/CIP1}$ inhibits initiator caspase cleavage by TRAIL death receptor DR4. Biochem Biophys Res Commun 2000;269:179–90.

50. Suzuki A, Tsutomi Y, Akahane K, Araki T, Miura M. Resistance to Fas-mediated apoptosis: activation of caspase 3 is regulated by cell cycle regulator $p21^{WAF1}$ and IAP gene family ILP. Oncogene 1998;17:931–9.

51. Steinman RA, Johnson DE. $p21^{WAF1}$ prevents down-modulation of the apoptotic inhibitor protein c-IAP1 and inhibits leukemic apoptosis. Mol Med 2000;6:736–49.

52. Hingorani R, Bi B, Dao T, Bae Y, Matsuzawa A, Crispe IN. CD95/Fas signaling in T lymphocytes induces the cell cycle control protein $p21^{cip-1/WAF-1}$, which promotes apoptosis. J Immunol 2000;164:4032–6.

53. Gartel AL, Radhakrishnan SK. Lost in transcription: p21 repression, mechanisms, and consequences. Cancer Res 2005;65:3980–5.

Mitogen-Activated Protein Kinase Kinase Inhibition Enhances Nuclear Proapoptotic Function of p53 in Acute Myelogenous Leukemia Cells

Kensuke Kojima, Marina Konopleva, Ismael J. Samudio, et al.

Cancer Res 2007;67:3210-3219.